Feasibility of white-light time-resolved optical mammography

Andrea Bassi
Lorenzo Spinelli
Cosimo D'Andrea
Arianna Giusto
ULTRAS-CNR-INFM and CNR-IFN
Politecnico di Milano
Dipartimento di Fisica
Piazza Leonardo da Vinci 32
20133 Milano, Italy

Johannes Swartling
University of Cambridge
Department of Chemical Engineering
New Museums Site, Pembroke Street
Cambridge, CB2 3RA, United Kingdom

Antonio Pifferi
Alessandro Torricelli
Rinaldo Cubeddu
ULTRAS-CNR-INFM and CNR-IFN
Politecnico di Milano
Dipartimento di Fisica
Piazza Leonardo da Vinci 32
20133 Milano, Italy

Abstract. We demonstrate the feasibility of white-light time-resolved optical mammography. The instrumentation is based on supercontinuum light generated in photonic crystal fiber and 32-channel parallel time-correlated single-photon-counting detection. Total measurement time is of the order of 10 min for typical clinical applications. Preliminary measurements performed on volunteers show the ability of the system to determine tissue constituent concentrations and structure over the entire breast area. Furthermore, measurements on a tissue-like sample demonstrate detection and characterization of inclusions.
© *2006 Society of Photo-Optical Instrumentation Engineers.* [DOI: 10.1117/1.2355663]

First proposed in the early 1990s, laser-based techniques for detection of breast cancer have since been steadily increasing in terms of rate of development. Like x-ray mammography, optical mammography is a noninvasive technique, but without the potential risks involved with the use of ionizing radiation. It is clear, however, that the spatial resolution of optical images is inferior to that obtained by x rays due to the strong scattering at optical wavelengths. Instead, the great potential for optical mammography lies in functional imaging, providing physiological information by spectrometric quantification of parameters such as tissue constituents and oxygenation. The wavelength region of choice is normally in the near infrared (NIR), where tissue absorption is relatively low and transmittance measurements are therefore feasible.

Several optical mammography instruments have been constructed for use in clinical studies.[1] Since the spectral information is a key issue in optical mammography images, the current generation of optical mammographs uses between two and seven wavelengths for analysis of the total hemoglobin content (THC), the oxygen saturation (StO_2), and in some cases water and lipid abundance. This also enables evaluation of the (1) scattering amplitude and (2) power, as defined by the formula $\mu_s' = a(\lambda/\lambda_0)^b$, where μ_s' is the reduced scattering coefficient, λ is the wavelength, and λ_0 is a fixed reference wavelength[2,3] (in our case 600 nm). The inclusion of more wavelengths would give additional spectral information that may be advantageous in several ways: primarily, by increasing robustness in the presence of noise, and catering to other possible chromophores in the tissue. This argument is further emphasized when considering future use of advanced analysis techniques such as 3-D image reconstruction, since such evaluation is even more noise sensitive owing to the ill-conditioned nature of multiparameter reconstruction. Moreover, measurements at different wavelengths can improve the detection of structures, such as lesions, in the breast.[4]

Increasing the number of wavelengths also goes hand in hand with recent theoretical developments aimed at direct spectral reconstruction of chromophore concentrations rather than the traditional method of evaluating the absorption and reduced scattering coefficients (μ_a and μ_s', respectively) for each wavelength independently.[5–8]

In this letter, we demonstrate that clinical time-resolved optical mammography over a continuous spectral range is feasible using novel pulse-light sources and detection techniques. Furthermore, the spectral characterization of inhomogeneities is shown, using a perturbation approach on tissue-like phantoms.

The mammography system collects projection images of the breast compressed between Plexiglas® plates. The light source is a Nd:YVO_4 (Millennia V, Spectra Physics) pumped Ti:sapphire laser (Tissa 50, CDP Systems) coupled into a photonic crystal fiber (PCF) (NL PCF-750, Crystal-Fibre) to generate a pulsed supercontinuum. The light is guided from the PCF by a 50-μm-core-diam graded-index fiber to a variable

Address all correspondence to Andrea Bassi, Dipartimento di Fisica, Politecnico di Milano, piazza Leonardo da Vinci 32, Milano, 20133 Italy; Tel: +39 0223996058; Fax: +39 0223996126; E-mail: andrea.bassi@fisi.polimi.it
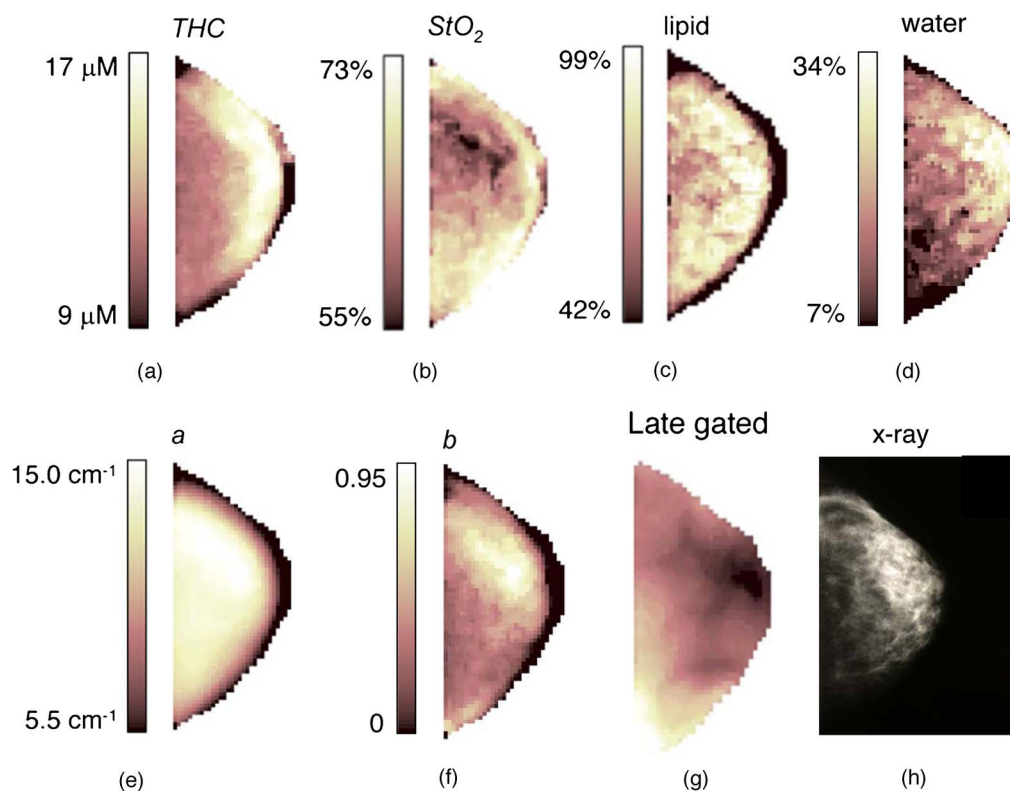
Fig. 1 Craniocaudal view of the left breast of healthy subject 1. Optically obtained images of (a) THC, (b) StO_2, (c) lipid, and (d) water, (e) and (f) *a* and *b* scattering parameters, (g) late-gated intensity image at 680 nm, and (h) x-ray mammogram.

neutral density filter and then illuminates the breast by means of a fiber collimator (F260FC, Thorlabs) that produces a 3-mm-diam beam. Part of the light is split off by a fused beamsplitter and used as a reference signal to monitor the temporal shape and amplitude of the light injected into the tissue.

A 3-mm fiber bundle collects the light on the opposite side of the breast. The bundle consists of seven plastic fibers (1-mm core) assembled circularly on the sample end and linearly on the detector end. One more fiber is added to the linear array for the reference signal. This part of the bundle is attached to an imaging spectrometer (SP-2150, Acton Research) coupled to a multianode 32-channel linear array photomultiplier tube (PMT) (R5900U-01-L32, Hamamatsu) sensitive up to 900 nm, and the spectral resolution is 9 nm/channel. A board for time-correlated single-photon counting (TCSPC) (SPC630, Becker & Hickl) and an in-house-built 32-channel router enables the simultaneous acquisition of 32 time-resolved curves. The system is optimized to acquire the signal between 606 and 885 nm, with an instrument response function of about 150 ps (FWHM). Both the light source and the detection stage were described and characterized in detail recently.[8,9] The scanning is automatically restricted to the breast area. Before the measurement, a procedure to detect the tissue border, based on feedback on the total photon count rate, is performed. The compressed breast is scanned with a spatial resolution of 2×2 mm^2 with an acquisition time of 312 ms/pixel. The photon count rate was limited by the TCSPC board to about 1 MHz in all measure-

ments and the power on the sample was chosen so as not to exceed this limit up to a maximum of 30 mW over the entire bandwidth. Since the light is projected on the sample over a 3-mm-diam area, the resulting power density is about 4 mW/mm^2, similar to that of other instruments for time-resolved optical mammography.[1]

Data were analyzed using a time-resolved spectrally constrained fitting approach recently developed by our group.[8] Briefly, the concentrations of oxyhemoglobin, deoxyhemoglobin, lipid, and water and the scattering *a* and *b* parameters are determined by minimizing the discrepancy between 32 theoretically calculated time-resolved curves and the 32 transmittance experimental curves.

Measurements were performed on the left and right breasts of three healthy volunteers. In Table 1 we report the age and the body mass index (BMI), the compressed breast thickness, and the scanned area. No selection of the volunteers was performed, meaning that the breast thickness and areas have representative values, typically found in mammography applications. However, they are younger in age compared to common patients.[10–12]

The acquisition time was chosen to obtain the highest photons count rate (to improve the SNR) with a short measurement time (to guarantee subject comfort). The count rates per pixel and the overall measurement times (including border detection and data saving) are also shown in Table 1. These times range between 4 and 12 min, similar to optical mammographs operating at a discrete number of wavelengths and compatible with clinical diagnostic procedure.

Table 1 From left to right: subject number, age, body mass index (BMI), left (L) or right (R) breast, compressed breast thickness, scanned area, photon counts per pixel, and overall acquisition time.

Subject	Age (yr)	BMI (kg/m^2)	Breast	Thickness (mm)	Area (mm^2)	Counts (kph/pixel)	Time (min:s)
1	53	23.8	L	50	5888	214	8:52
			R	48	6144	226	9:51
2	31	20.1	L	32	2532	307	4:17
			R	30	2848	253	4:25
3	27	20.0	L	36	7548	229	11:27
			R	39	8152	187	11:50

The breast constituents and structural parameters recovered on subject 1, left breast, are presented in Figs. 1(a) to 1(f), where typical values (indicated by the limits of the color bars) are found.[10–12] The images do not exhibit main structures because the three volunteers are healthy, and also because the model adopted in the fitting procedure assumes a homogeneous medium. We observe a region of higher THC in proximity of the areola. This is probably due to the compression that is stronger at the breast center, resulting in a displacement of blood near the tissue border.[13,14] Figure 1(g) shows instead that the presence of veins can be deduced gating the intensity at a late delay[4] at a single wavelength (here it is 680 nm). This method is often used to determine the presence of lesions in the breast. In a previously recorded radiographic image—Fig. 1(h)—we observe the presence of a high-density structure, the mammary gland, individuated by a white uneven structure. Visual comparison between the radiographic and water images reveals a positive correlation between the density and the water content. This is in agreement with the fact that water is a source of contrast in the radiographic images. The same behavior is found for the b scattering parameters. As in other works,[15,16] higher values of b are found in tissues with higher water content. The image quality is lower for water and lipid since in this spectral range the absorption is dominated by the hemoglobin. Future inclusion of longer wavelengths, where absorption peaks are well defined for lipid (at 930 nm) and water (975 nm), can be ad-

vantageous to decrease the noise in the measurement of these constituents.

Breast bulk properties are presented in Table 2, as the median values of the parameters over a wide reference area of the breast, far away from the boundaries. Furthermore, in Fig. 2 the bulk absorption [Fig. 2(a)] and scattering [Fig. 2(b)] spectra for both breasts of the three subjects are reported. Differences in the lipid and water concentrations are clearly visible in the absorption spectra. It is possible to identify a lipid rich breast tissue (subject 1, presence of an absorption peak at 930 nm in the spectra of both breasts) and a water-rich breast tissue (subject 2, high absorption at 975 nm for both breasts). On the other hand, absorption spectra of subject 3 are in between. From values reported in Table 2, we see also that the sum of lipid and water is between 70 and 90%. The additional content could be attributed to the presence of other tissue components (e.g., proteins) not considered in the fit. Moreover, high water content is related to high scattering power. Conversely high lipid content is found in tissue with low b. These features are in agreement with results obtained in a past clinical trial of over more than 150 subjects[12] and in high-accuracy spectroscopic data.[16] On the other hand, blood oxygenation of subject 3 is close to 40%, significantly below average values. Further investigation is required to elucidate this effect.

To demonstrate the ability of the system to characterize abnormalities in the tissue, five additional scans were carried

Table 2 Bulk total hemoglobin content (THC), blood oxygen saturation (StO$_2$), water and lipid content, scattering amplitude (a) and power (b) for the three volunteers, left (L) and right (R) breast.

Subject	Breast	THC (μM)	StO$_2$ (%)	Lipid (%)	Water (%)	a (cm^{-1})	b
1	L	12.5	61.9	77.3	16.5	13.4	0.45
	R	12.1	57.3	79.4	13.9	12.5	0.32
2	L	14.0	68.4	33.1	30.8	15.5	0.56
	R	14.5	62.2	34.4	35.8	17.0	0.73
3	L	9.9	37.9	61.5	23.1	20.9	0.32
	R	10.4	39.6	59.5	24.0	19.3	0.37

Table 3 Ink concentrations of inclusion (expected and measured) and background.

	Blue-Black Concentration (%)				
	0–100	25–75	50–50	75–25	100–0
Expected	0–100	25–75	50–50	75–25	100–0
Measured	0.0–100.0	13.3–86.7	47.2–52.8	74.1–25.9	100.0–0.0
Background	51.1–48.9	50.7–49.3	47.3–52.7	50.2–48.8	53.0–47.0

on 50-mm-thick liquid phantoms, constituted by a background and spherical inclusion ($\sim$1 cm^3), placed in the middle. The background is made of water, Intralipid$^{\circledR}$, and a mixture of equally concentrated blue and black inks (Rotring, characterized elsewhere[8]) to have $\mu_a = 0.1$ cm^{-1} and $\mu_s' = 10$ cm^{-1} at 660 nm. The inclusion—contained in a transparent film—is made of the same substances but the absorption is about 3 times higher. The relative concentration of blue and black inks in the inclusion is varied within the five measurements: the blue ink is increased from 0 to 100% in 25% steps and the black is decreased correspondingly (the percentage refers to

the total quantity of inks). Measurements were analyzed using a perturbation approach for time-resolved transmittance based on the diffusion approximation to determine the absorption and scattering coefficients.[17] The method is applied to all the available wavelengths and the recovered absorption spectrum is further interpreted as the linear combination of the inks and water absorption, giving their concentration. The result of the fitting is presented in Table 3. The expected and calculated relative concentrations of blue-black ink in the inclusion are shown on lines 1 and 2, respectively; the calculated concentration of the background (expected to be 50% blue and 50% black in all measurements) is shown on line 3. The table shows that the concentration of the inks is determined with a maximum difference between the expected and measured value of 12%.
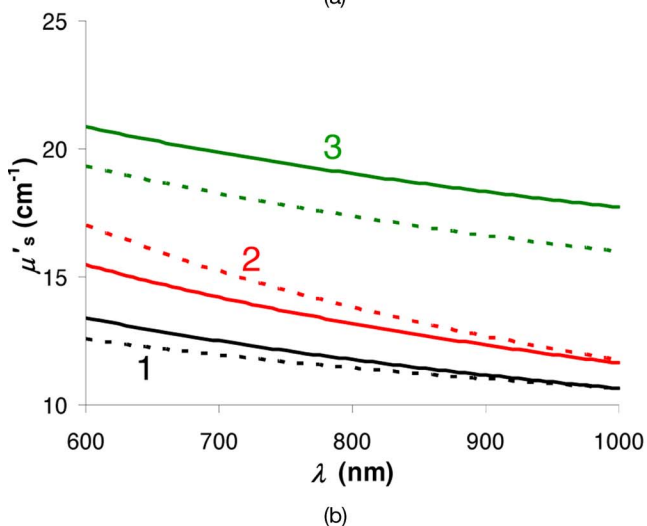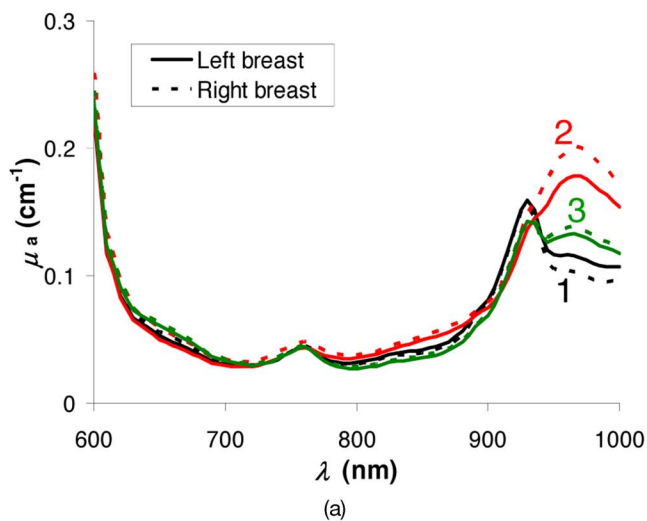
In conclusion we presented a step toward the achievement of spectral and time-resolved optical mammography in clinical environment. For better portability, the light source can be substituted for with a compact pulsed supercontinuum source, recently commercially available.[18] The acquisition time (currently about 10 min per projection) can be further reduced by using TCSPC systems with multichannel capability.[19]

Fig. 2 (a) Bulk absorption and (b) scattering spectra for both left (solid lines) and right (dashed lines) breasts for three subjects.

References

1. For recent reviews on optical mammography see *Phys. Med. Biol.* **50** (2005) and *Technol. Cancer Res. Treat.* **4** (2005).
2. J. R. Mourant, T. Fuselier, J. Boyer, T. M. Johnson, and I. J. Bigio, "Prediction and measurement of scattering and absorption over broad wavelength ranges in tissue phantoms," *Appl. Opt.* **36**, 949–957 (1997).
3. A. M. Nilsson, K. C. Sturesson, D. L. Liu, and S. Addersson-Engels, "Changes in spectral shape of tissue optical properties in conjunction with laser-induced thermotheraphy," *Appl. Opt.* **37**, 1256–1267 (1998).
4. P. Taroni, L. Spinelli, A. Torricelli, A. Pifferi, G. M. Danesini, and R. Cubeddu, "Multi-wavelength time domain optical mammography," *Technol. Cancer Res. Treat.* **4**, 527–537 (2005).
5. A. Li, Q. Zhang, J. P. Culver, E. L. Miller, and D. A. Boas, "Reconstructing chromosphere concentration images directly by continuous-wave diffuse optical tomography," *Opt. Lett.* **29**, 256–258 (2004).
6. S. Srinivasan, B. W. Pogue, S. Jiang, H. Dehghani, and K. D. Paulsen, "Spectrally constrained chromophore and scattering near-infrared tomography provides quantitative and robust reconstruction," *Appl. Opt.* **44**, 1858–1869 (2005).
7. A. Corlu, T. Durduran, R. Choe, M. Schweiger, E. M. C. Hillman, S. Arridge, and A. G. Yodh, "Uniqueness and wavelength optimisation in continuous-wave multispectral diffuse optical tomography," *Opt. Lett.* **28**, 2339–2341 (2003).

8.   C. D'Andrea, L. Spinelli, A. Bassi, A. Giusto, D. Contini, J. Swartling, A. Torricelli, and R. Cubeddu, "Time-resolved spectrally constrained method for the quantification of chromophore concentrations and scattering parameters in diffusing media," *Opt. Express* **14**, 1888–1898 (2006).

9.   A. Bassi, J. Swartling, C. D'Andrea, A. Pifferi, A. Torricelli, and R. Cubeddu, "Time-resolved spectrophotometer for turbid media based on supercontinuum generation in a photonic crystal fiber," *Opt. Lett.* **28**, 2405–2407 (2004).

10.   T. Durduran, R. Choe, J. P. Pulver, L. Zubkov, M. J. Holboke, J. Giammarco, B. Chance, and A. G. Yodh, "Bulk optical properties of healthy female breast tissue," *Phys. Med. Biol.* **47**, 2847–2861 (2002).

11.   D. Grosenick, K. T. Moesta, H. Wabnitz, J. Mucke, C. Stroszczynski, R. Macdonald, P. M. Schlag, and H. Rinneberg, "Time-domain optical mammography: initial clinical results on detection and characterization of breast tumors," *Appl. Opt.* **42**, 3170–3186 (2003).

12.   L. Spinelli, A. Torricelli, A. Pifferi, P. Taroni, G. M. Danesini, and R. Cubeddu, "Bulk optical properties and tissue components in the female breast from multiwavelength time-resolved optical mammography," *J. Biomed. Opt.* **9**(6), 1137–1142 (2004).

13.   S. Jiang, B. W. Pogue, K. D. Paulsen, C. Kogel, and S. Poplack, "*In vivo* near-infrared spectral detection of pressure-induced changes in breast tissue," *Opt. Lett.* **28**, 1212–1214 (2003).

14.   S. Carp, T. Kauffman, Q. Fang, E. Rafferty, D. Kopans, and D. Boas, "Compression induced changes in the physiological state of the breast as derived from combined frequency domain photon migration and white light spectroscopy measurements," in *Biomedical Optics 2006 Technical Digest*, Optical Society of America, Washington, DC (2006).

15.   A. E. Cerussi, D. Jakubowski, N. Shah, F. Bevilacqua, R. Lanning, A. J. Berger, D. Hsiang, J. Butler, R. F. Holcombe, and B. J. Tromberg, "Spectroscopy enhances the information content of optical mammography," *J. Biomed. Opt.* **7**, 60–71 (2002).

16.   A. Pifferi, J. Swartling, E. Chikoidze, A. Torricelli, P. Taroni, A. Bassi, S. Andersson-Engels, and R. Cubeddu, "Spectroscopic time-resolved diffuse reflectance and transmittance measurements of the female breast at different interfiber distances," *J. Biomed. Opt.* **9**, 1143–1151 (2004).

17.   L. Spinelli, A. Torricelli, A. Pifferi, P. Taroni, and R. Cubeddu, "Experimental test of a perturbative model for time-resolved imaging in diffusive media," *Appl. Opt.* **42**, 3145–3153 (2003).

18.   www.koheras.com, www.fianium.com.

19.   www.becker-hickl.de.